Earthquakes and Structures, *Vol. 15, No. 4 (2018) 351-360*
DOI: https://doi.org/10.12989/eas.2018.15.4.351

Energy based design of a novel timber-steel building

Caleb Goertz[1], Fabrizio Mollaioli[*2] and Solomon Tesfamariam[3]

[1]*Read Jones Christoffersen Ltd., Victoria, BC, Canada*
[2]*Department of Structural and Geotechnical Engineering, Sapienza University of Rome, Via Gramsci 53, 00197 Rome, Italy*
[3]*School of Engineering, University of British Columbia, 3333 University Way, Kelowna, BC, Canada*

(Received November 9, 2017, Revised March 23, 2018, Accepted April 18, 2018)

Abstract. Energy-based methodology is utilized to design novel timber-steel hybrid core wall system. The timber-steel core wall system consists of cross laminated timber (CLT), steel columns, angled brackets and t-stub connections. The CLT wall panels are stiff and strong, and ductility is provided through the steel t-stub connections. The structural system was modelled in SAP2000 finite element program. The hybrid system is explained in detail and validated using first principles. To evaluate performance of the hybrid core system, a 7-story building was designed using both forced-based design and energy based design (EBD) approaches. Performance of the structure was evaluated using 10 earthquakes records selected for 2500 return period and seismicity of Vancouver. The results clearly served as a good example of the benefits of EBD compared to conventional forced based design approaches.

Keywords: energy-based design; hybrid system; cross laminated timber; connection

1. Introduction

With introduction of mass timber, such as cross laminated timber (CLT), tall wood buildings have become popular in Canada and other part of the world (e.g., Smith and Frangi 2014, Pei *et al*. 2014, Green and Karsh 2012). Advantages of mass-timber building are: lower carbon footprint, constructability, aesthetics and reduced construction time. In this paper, a new timber-steel hybrid structural system is proposed (Fig. 1). The hybrid system entails use of timber-core wall system using CLT panels to resist lateral loads and steel columns with ductile connection to dissipate energy (Goertz 2016). In addition, the hybrid building was designed using energy-based design (EBD). This paper gives details of the hybrid building and implementation of EBD.

Mass timber products have high strength and low ductility, consequently, often result in brittle failure. Inelastic deformation in CLT buildings is controlled by connections (e.g., Schneider *et al*. 2014, Rinaldin *et al*. 2013). To increase building height further, while satisfying code-safety requirement, hybrid buildings are viable option (e.g., Tesfamariam *et al*. 2015). Advantages of using steel-timber hybrid building were reported by various authors (e.g., López-Almansa *et al*. 2015, Zhang *et al*. 2015, Dickof *et al*. 2013). Stiemer *et al*. (2012), Dickof (2013) developed novel hybrid steel-timber system, by coupling steel moment resisting frame and CLT infill walls. Tesfamariam *et al*. (2014) showed potential of this building type in high seismic region by carrying out probabilistic seismic vulnerability assessment. For this hybrid system, an equivalent viscous damping and direct displacement based design was developed (Bezabeh *et al*. 2015a, b, Bezabeh 2014). Dickof *et al*. (2014) quantified ductility and overstrength factors using static pushover analysis. Tesfamariam *et al*. (2015), Bezabeh *et al*. (2017) developed overstrength and ductility factors using FEMA P695 (FEMA 2009).

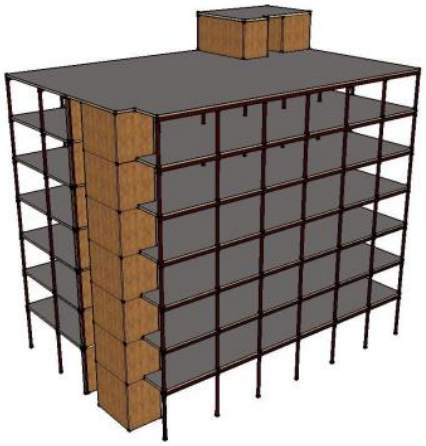

Fig. 1 Proposed steel-CLT hybrid building

Performance-based seismic design (PBSD) provides design guidelines that enable designers meet a predetermined performance level (FEMA 2009, Pang and Rosowsky 2009, Ghobarah 2001, SEAOC Vision 2000 Committee 1995). Performance of the building can be defined with acceleration and/or drift limits, for specified ground motion intensities. In this paper, the EBD, within the framework of PBSD is considered. Energy based design involves defining seismic loads in energy term, and determining energy absorption and dissipation capacity of the structure (Akiyama 1985, Uang and Bertero 1990,

∗Corresponding author, Professor
E-mail: fabrizio.mollaioli@uniroma1.it

ISSN: 2092-7614 (Print), 2092-7622 (Online)

Decanini and Mollaioli 1998, 2001). The energy accounts for the frequency content, amplitude, duration of strong motion, and consequently the cumulative inelastic action of structure (e.g., Leelataviwat *et al*. 2002, Benavent-Climent 2011).

2. Evolution of energy based design

The EBD's first step is characterization of the energy demand (Cheng *et al*. 2014, 2015), for a selected performance level, to establish the energy dissipation capacity that should be provided in the structure. Once the demand is known, the second step consists in the design of the structure so as to supply the energy necessary to balance the demand. For the EBD, equation of motion (Eq. (1)) is integrated with respect to u (relative displacement) to define the equation in energy terms (Eq. (2)).

$$m\ddot{u} + c\dot{u} + ku = -m\ddot{u}_g \tag{1}$$

where m=the mass of the system, c=viscous damping coefficient, k=stiffness, u=relative displacement, and u_g=ground acceleration. By integrating each term with respect to u, the equation of motion in energy terms can be derived as

$$\int m\ddot{u}\,du + \int c\dot{u}\,du + \int ku\,du = -\int m\ddot{u}_g\,du \tag{2}$$

The three terms on the left side of Eq. (2) are related to the structural characteristics and represent the stored kinetic energy (E_K), dissipated energy through damping (E_D), and absorbed energy (E_A). The absorbed energy can be further separated into strain energy (E_S) and hysteretic energy dissipation (E_H). The strain energy represents the recoverable energy that the structure can withstand whereas the hysteretic energy represents the irrecoverable hysteretic energy which causes the damage to the structure. These energies, when summed equate to the total input energy subjected by the earthquake (E_I). Therefore, the energy equation can be simplified as

$$E_K + E_D + E_S + E_H = E_I \tag{3}$$

Various energy-based design methodologies are reported in the literature (e.g., Donaire-Avila *et al*. 2017, Benavent-Climent 2011, Ghosh *et al*. 2009, Choi and Kim 2005, 2009, Leelataviwat *et al*. 2002). The fundamental concept of EBD is the energy-balance concept (e.g., Leelataviwat *et al*. 2002, Choi and Kim 2005, 2009, Ghosh *et al*. 2009) is shown in Fig. 2. Fig. 2 shows that the elastic and plastic energy when summed should equate to the input energy of an equivalent elastic system at the maximum target displacement (Choi *et al*. 2006). These studies displayed that the target performance was met when the designs were subjected to analytical design earthquakes.

3. CLT-steel hybrid building

3.1 System configuration

A 7-story residential reinforced concrete (RC) building

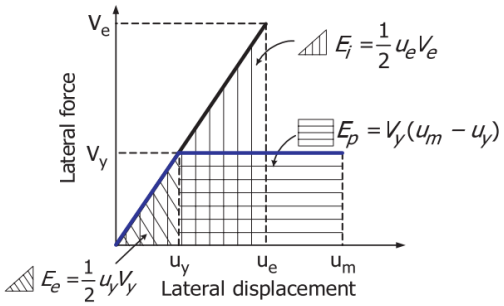

Fig. 2 Energy balance concept with force-displacement relationship (modified after Choi *et al*. 2006)

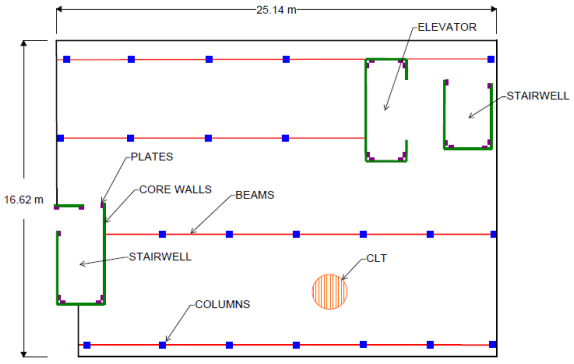

(a) Floor plan

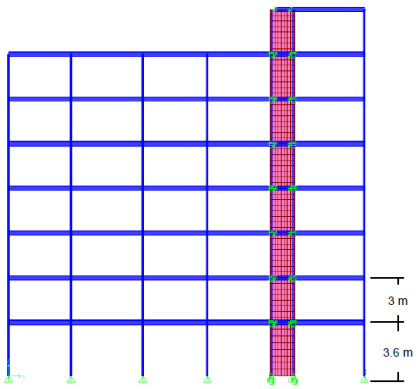

(b) Elevation view

Fig. 3 Steel-timber hybrid building

located in Vancouver, Canada, was used as benchmark building (Fig. 1, Fig. 3). The RC building, however, was re-designed as CLT core wall system with steel columns. The floor plan shown in Fig. 3(b) was kept uniform for the seven floors. A mechanical room was added to the roof level (Fig. 3(b)) similar to the benchmark RC building. The height of the first and subsequent stories are 3.6 m and 3m, respectively, resulting in the total building height (including the mechanical roof top room) of 24.6 m (Fig. 3(b)).

Steel beams were designed to transfer the gravity loading from the timber floor panels to the steel columns. Connecting two different building materials is challenging in any system and requires more detail than typical connections. Much research recently has focused on timber-steel connections (e.g., Asiz and Smith 2011, Loss *et al*. 2014, Schneider *et al*. 2014, Shen *et al*. 2013). Experiments were conducted in Italy (Loss *et al*. 2014, Loss *et al*. 2015a,

2015b) to determine the behaviour of CLT panels secured to wide flange steel beams.

The study considered several different connections between the beam and panel and the results were presented and discussed. Most notably test # five in their study considered inclined screws into the CLT panels from angles that were welded to the steel beam. The results showed ductile behaviour of the connections between the steel beam and CLT panel after yielding. The connection between the steel beam and floor panels, however, was designed to remain elastic; therefore, the connection was not studied in detail for this research.

A simple load bearing connection was proposed for the connection between the steel beam and steel column. The connection was designed to stay well within the elastic range and transfer the axial and shear forces from the beam to the columns. Numerical values for the connection were taken from the Canadian Institute of Steel Construction (CISC) Handbook (CISC 2010).

There are a few instances in the designed building where a steel beam connects with a CLT core wall panel. To transfer the loads between the two elements an end plate was proposed. The end plate would be welded to the steel beam and use high strength screws placed at an angle using the angled wedge washers. This connection would transfer the necessary shear forces to the CLT shear wall.

3.2 Modeling of lateral and gravity loading resisting systems

To validate the seismic design of the building, finite element software is used by structural engineers to predict the response. The analysis was carried out using the SAP2000 commercial finite element software developed by Computers and Structures Inc. (CSI 2013). In this section a description of the adopted model for each structural element is discussed.

Usually, orthotropic CLT panels are manufactured using odd numbered layers; currently 3, 5, 7, and 9 layer and are available for production by the most popular CLT manufacturers (KLH 2012, Structurlam 2013). For this reason, even though the strength in each layer is the same, with an odd number of layers there is always one more layer in one direction making it the stronger direction. The CLT panels were modeled as orthotropic shell elements. To determine the modulus of elastic and shear moduli of the CLT panel in all planes the '*k* Method' was used from the CLT Handbook (Blass and Fellmoser 2004). The *k* factors depend on the Young's modulus or shear modulus in the considered direction and at ninety degrees to the direction considered.

Following the Structurlam design guide the Young's modulus and shear modulus were developed in each direction according to the composite theory, '*k* Method'. The initial values for Young's modulus and shear modulus from the manufacturer were multiplied by the *k* factor which equated to the properties in their respective direction (Blass and Fellmoser 2004).

In this building 5 and 7 layer CLT panels were designed. SAP2000 uses three node triangular elements or four node quadrilateral elements to solve finite element shell problems (CSI 2013). However, the four node quadrilateral elements are more accurate and will be used in this study as all elements are rectangular. The shell's stiffness is calculated using 2x2 Gauss integration points and then extrapolated on to the element joints.

Table 1 Orthotropic CLT properties

Young's Modulus	Shear Modulus
E_0=9500 MPa	G_0=950 MPa
E_{90}=317 MPa	G_{90}=50 MPa
5 Layer	
E_1=3794 MPa	G_1=379 MPa
E_2=6022 MPa	G_2=602 MPa
E_3=258 MPa	G_3=41 MPa
7 Layer	
E_1=4275 MPa	G_1=428 MPa
E_2=5539 MPa	G_2=554 MPa
E_3=231 MPa	G_3=36 MPa

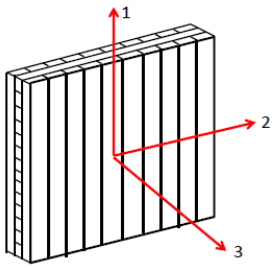

Following the '*k* Method' the orthotropic properties were developed and are summarized in Table 1. The *k* factors were computed using the elastic and shear modulus in both parallel (E_0, G_0) and perpendicular (E_{90}, G_{90}) directions.

All steel members were input to the model using the SAP2000 database for Canadian steel members. However, the plates were input to the model through the section designer provided in SAP2000. The frame members were discretized according to the accuracy necessary for the study. Anyway, the meshing of the steel members has shown to have a small effect on the results, so a larger mesh size was appropriate to save computing effort.

Accurately modeling the connections is the most critical detail in the analysis of the steel-timber hybrid building and dictates whether the obtained results were correct. With extensive research into the program analysis methods the connections were modeled appropriately. Using experimental tests the connections were validated using SAP2000 and then compared with experimental work. Elastic and nonlinear spring elements were utilized in the building model.

Two node spring elements were used within the analytical model to depict the behaviour of the steel connections between the CLT shear wall and steel plate and CLT wall to door connection. Linear and multilinear plastic springs were used depending on the connection strength and role in the building.

Nonlinear plastic springs significantly slow down the computation time and therefore linear elastic springs were used to simplify connections that do not play a large role in

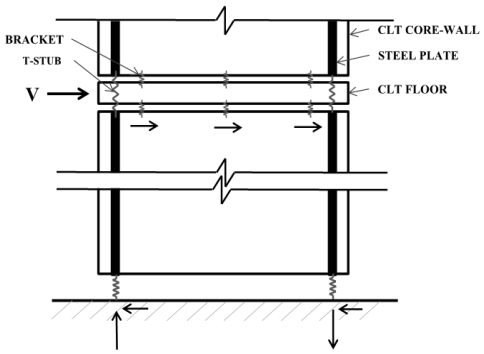

Fig. 4 Schematic of the proposed timber-steel core system

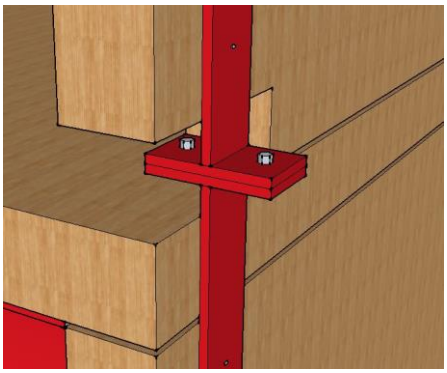

Fig. 5 Rendering of the *t*-stub connection

the lateral behaviour of the building. Moreover, the elastic springs were designed to remain elastic and therefore do not require the nonlinear design. Furthermore, the spring properties changed based on the global coordinates so two defined springs are required for the 3D analytical model.

A schematic of the proposed hybrid system that couples the light and stiff CLT walls with steel plates and ductile steel connections is shown in Fig. 4. The steel plates are designed to run the height of the wall and fastened to the CLT wall panel with screws. These walls were connected at the intersection of each floor by t-stub connections that are bolted together as shown in Fig. 5. The core walls are designed as a platform construction method that allows for a safe floor to work on while installing the next floor, saving money and time. As the figure shows, the steel plates were not connected to the floors as the floors connect to the core walls with brackets and hold-down connections. The seismic forces were transferred to the core wall through the diaphragm and thus the connections of the diaphragm to the core walls.

The t-stub connection (shown Fig. 5) controls the inelastic deformation of the building. This t-stub connection was designed by end steel plates and were connected by high strength 27 mm diameter bolts (Piluso *et al*. 2001). Piluso *et al*. (2001) studied this *T*-stub connection and validated their theoretical equation through experimental work. Under seismic action all other components of the building design were designed to remain elastic while the *t*-stub is designed to behave plastically. Therefore, the *t*-stub connection dissipated the seismic force and controls ductility of the hybrid system.

The connection is stiff until the yield point and exhibits

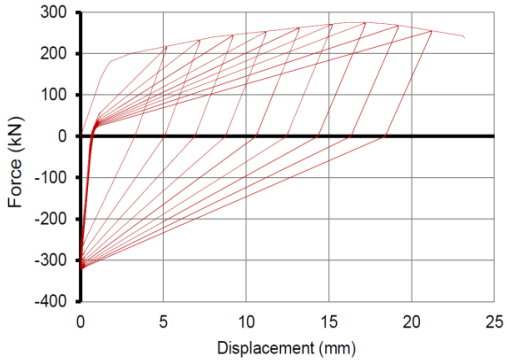

Fig. 6 Force-displacement curve pivot model in SAP2000 for *t*-stub connection cyclic tests. The multilinear plastic behaviour was used to allow for the plastic behaviour in the connection

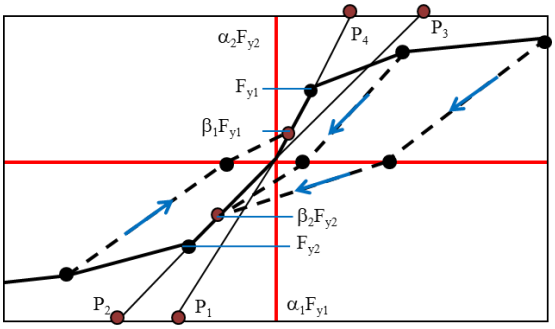

Pivot model parameters	
α_1	50
α_2	10
β_1	0.1
β_2	0.7

Fig. 7 SAP2000 pivot model

a ductile behavior (Fig. 6). Cyclic tests conducted by Piluso and Rizzano (2008) showed no negative deformation, as the *t*-stub connection is extremely stiff in compression due to the contact between the two steel plates. The hysteretic behavior of the *t*-stub connection, for the experimental result reported by Piluso and Rizzano (2008), was modelling in SAP2000 (CSI 2006) using a pivot model (Dowell *et al*. 1998) and the result is shown in Fig. 6.

SAP2000 provides three different hysteresis types for the multilinear links: kinematic, Takeda and pivot. The hysteresis of *t*-stub connections from experimental tests showed to be most similar to the pivot hysteresis type. The model was developed by Dowell *et al*. (1998) for reinforced concrete members. However, the hysteresis quite accurately predicted the response of the *t*-stub connection. The pivot model allowed the researchers to modify the curve using the variables in the model to tweak the curve to better capture the behavior of the *t*-stub connection (Fig. 7). A detailed discussion on the pivot method and variables can be found in Dowell *et al*. (1998).

SAP2000 does not fail a nonlinear spring during analysis when the final connection strength is reached. Once the springs reach the final nonlinear point in the defined curve they continue on with the same strength rather than failing. In this thesis, however, under dynamic

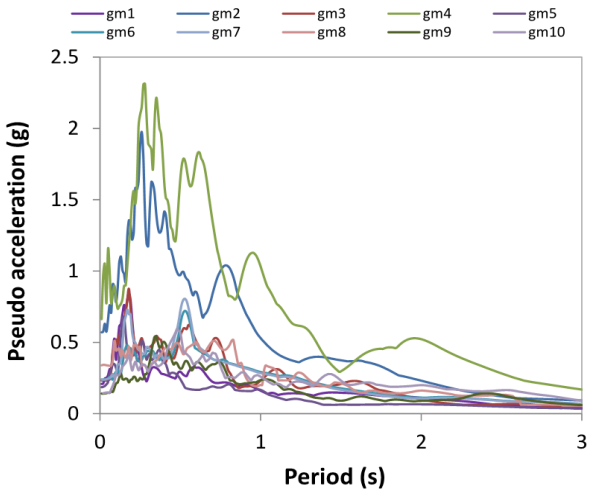

Fig. 9 Pseudo acceleration response spectra

analysis the *t*-stub connections do not reach the failure point. However, if pushover analysis was conducted manual post-processing would be required to determine the failure point of the system.

The steel plates, columns and beams were assigned frame properties in SAP2000. Nonlinearity in the frame member is possible through frame hinges in SAP2000; however, the steel-timber hybrid being analyzed does not require hinges as the steel columns and beams were not designed to transfer moments and resist the lateral force due to an earthquake. The steel plates in the core system were designed as part of the lateral system but do not require plastic hinges as the links account for the nonlinear behaviour of the *t*-stub connection and plate.

Frame releases were used to not allow the beam-column connections to transfer moments. All the columns ends were set to transfer zero moment and the frames were continuous with the CLT floor panels.

4. Methodology of the energy based design

In this paper, by modifying Choi *et al*. (2006), an 11-step procedure is proposed (Fig. 8). Fig. 8 shows flowchart for the EBD methodology used in the steel-timber core wall system. A step-by-step implementation of the proposed method is shown below.

Step 1: Select earthquake records

Earthquake records were selected for seismicity of Vancouver, and consideration of soil class C (Fig. 9). The ground motions were selected using a multiple-conditional-mean-spectra method (Atkinson and Goda 2011, Baker 2011). The records do not take into account the presence of long duration pulses due to forward directivity effects. The pseudo acceleration and velocity spectra were developed using the program Bispec (Hachem 2004). Bispec is a nonlinear spectral analysis software that uses earthquake ground motion records to perform uni-directional and bi-directional dynamic time history analysis on single degree of freedom (SDOF) systems.

Step 2: Determine target displacement and ductility ratio

This EBD methodology relies on a target displacement (u_T) to compute ductility ratio (μ_T) based off known yield displacement (u_y) of the system. Target drift are set based on the structure type and desired performance level (Ghobarah 2001). The u_y is obtained for the steel-timber hybrid system without accounting the inelastic behaviour of connections. The target ductility ratio is then defined as the target to yield drift

$$\mu_T = \frac{u_T}{u_y} \tag{4}$$

For the timber-steel hybrid system the interstory drift was limited to 2% as this would result in an overall drift of 1.5% to meet the life safe performance level (Ghobarah 2001). Therefore, the yield drift of the system was found to be 143 mm and the target drift was set as 369 mm. These drifts resulted in a target ductility of 2.5.

Step 3: Convert the MDOF structure to an equivalent SDOF structure

The yield and target displacement are then used to derive the equivalent SDOF yield ($u_{y,eq}$) and target displacement ($u_{T,eq}$) (ATC 1996)

$$u_{T,eq} = \frac{u_T}{\Gamma_1 \Phi_{t1}} \tag{5}$$

$$u_{y,eq} = \frac{u_y}{\Gamma_1 \Phi_{t1}} \tag{6}$$

where Γ_1=modal participation factor and Φ_{t1}=fundamental mode shape vectors roof story component.

Step 4: NLTHA on SDOF structure

Based on constant ductility, nonlinear time history analysis (NLTHA) was carried out on the SDOF structure with a bi-linear force displacement relationship. Damping is assumed to be 5% of the critical damping. A period range of 0.01 to 3.0s is used to compute the acceleration, velocity and energy spectra.

Step 5: Determine period

To compute the fundamental period, for the first iteration of the methodology, empirical formula from the NBCC for shear walls is used (Eq. (7)). Subsequently, the fundamental period will be re-iterated until convergence is achieved.

$$T = 0.05(h_n)^{3/4} \tag{7}$$

where h_n=height of the structure (m).

Step 6: Compute the input energy

The input energy (E_I) is estimated using the energy-balance concept as

$$E_I = \frac{1}{2} M_1 S_v^2 = \frac{1}{2} M_1 \left(\frac{T_1 S_a}{2\pi} \right)^2 \tag{8}$$

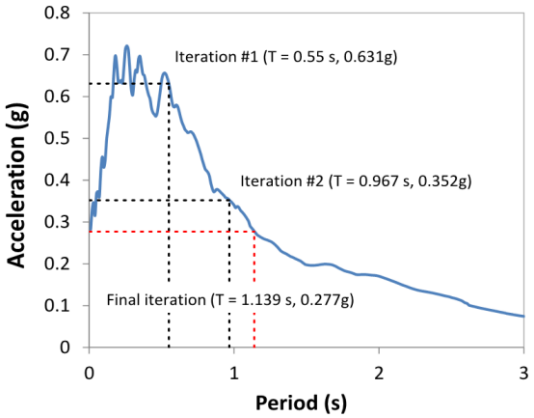

Fig. 10 Average acceleration for each trial period

where M_1=first modal mass, S_v=pseudo velocity and S_a=pseudo acceleration.

This study uses the pseudo acceleration to estimate the input energy. The pseudo acceleration in determining the input energy is obtained by taking the average pseudo acceleration of the 10 ground motions. It should be noted that the average value have the following two drawbacks: (i) the design plot is not smoothened, thus containing peaks and valleys that are not representative of a sufficiently wide set of inputs, and (ii) given the individual spectra are highly scattered (Fig. 9). This study should be extended considering representative percentile (i.e., 95%) to provide provided more uniform probability of exceedance. The average acceleration of the ten ground motion records is shown in Fig. 10 along with the design iterations.

The estimate of input energy has shown to underestimate the earthquake energy input to the structure (Choi *et al*. 2006). Therefore, Choi *et al*. (2006) recommend a modification factor (α) to estimate the correct input energy (E_i*)

$$\alpha = \left(\frac{E_{i,inelastic}}{E_{i,elastic}}\right)\left(\frac{V_{eq}}{S_v}\right)^2 \tag{9}$$

where ($E_{i,inelastic}/E_{i,elastic}$)=ratio of inelastic to elastic input energy for the target ductility and V_{eq}=equivalent velocity and is computed as

$$V_{eq} = \sqrt{\frac{2E_i}{m}} \tag{10}$$

The equivalent velocity is plotted using the above equation in Fig. 11(a). Furthermore, the inelastic to elastic input energy ratio is plotted in Fig. 11(b). The E_i* is computed as

$$E_i^* = \alpha E_i \tag{11}$$

Step 7: Compute the yield base shear and elastic energy

The yield base shear (V_y) and elastic energy (E_e) are then computed as

$$V_y = \frac{E_i^*}{u_{T,eq}\left(1-\frac{1}{2\mu}\right)} \tag{12}$$

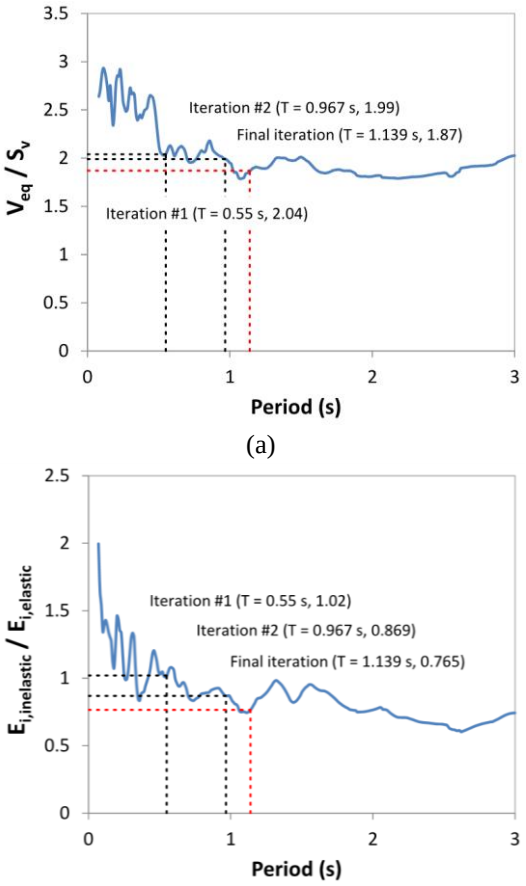

(a)

(b)

Fig. 11 Ratio of (a) the equivalent velocity to pseudo velocity; (b) inelastic to elastic input energy

$$E_e = \frac{1}{2}u_{y,eq}V_y \tag{13}$$

Step 8: Compute the plastic energy demand

Finally, the plastic energy demand for the inelastic system (E_p^*) is estimated

$$E_p^* = \beta\left(E_i^* - E_e\right) \tag{14}$$

where β=correction factor to account for the overestimation of hysteretic energy ratio and is computed as (Choi *et al*. 2006)

$$E_p^* = \frac{E_h/E_i}{E_p/E_i} \tag{15}$$

where E_h=hysteretic energy and found through the NLTHA in step 5. The ratio of hysteretic to input energy is plotted in Fig. 12.

The plastic energy demand must now be modified for the MDOF E_{pM}^* structure as

$$E_{pM}^* = \gamma E_p^* \tag{16}$$

where γ=ratio of plastic energy for a MDOF to an equivalent elastic SDOF ($E_{P,MDOF}/E_{P,ESDOF}$).

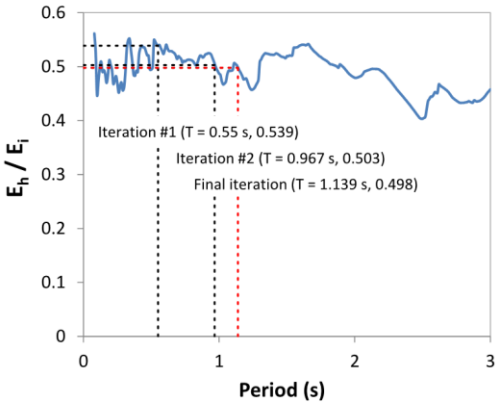

Fig. 12 Hysteretic to input energy ratio

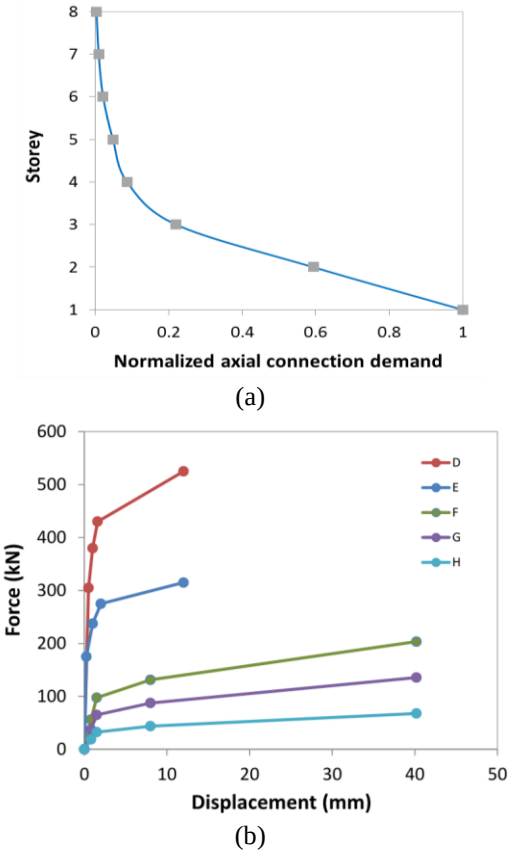

Fig. 13 (a) Normalized axial distribution ratio; and (b) Force-displacement diagram of the *T*-stub connections for 2D EBD

Step 9: Distribute plastic energy based on shear distribution

The energy distribution was determined for the proposed system according to the *t*-stub connections. Therefore, the axial distribution was the best representative for the dissipation of energy. The 2D structure designed using ESFP is analyzed using NLTHA to determine the energy distribution. The results for each earthquake are averaged to determine the final distribution (Fig. 13(a)). The displayed axial connection demand (Fig. 13(a)) are referred to the roof that include the mechanical room. The plastic energy demand from step 8 was then applied to the structure

Table 2 EBD process for timber-steel hybrid structure with 1.5% target drift

	Design iterations			
Parameters	1	2	···	Final
Period (s)	0.550	0.967	···	1.139
Acceleration (g)	0.631	0.352	···	0.277
E_i (kN·mm)	902.8	874.9	···	740.1
V_{eq} / S_v	2.040	1.990	···	1.870
$E_{i,inelastic} / E_{i,elastic}$	1.020	0.869	···	0.765
Ei^* (kN·mm)	3832.0	3010.7	···	1979.8
V_y (kN)	20.715	16.400	···	10.516
E_h / E_i	0.539	0.503	···	0.498
$(E_h / E_i) / (E_p / E_i)$	0.710	0.663	···	0.656
$E_{p,MDOF} / E_{p,SDOF}$	0.759	0.759	···	0.759
E_{pM}^* (kN·mm)	1563.8	1146.6	···	746.5
T-stub$_7$	G	G	···	H
T-stub$_6$	G	G	···	H
T-stub$_5$	G	G	···	H
T-stub$_4$	G	G	···	H
T-stub$_3$	G	G	···	H
T-stub$_2$	F	G	···	H
T-stub$_1$	D	E	···	E

according to the distribution and the connections are designed to dissipate this energy. Limiting factors on the connection design are the resulting interstory drift and maximum displacement. The *t*-stub connections used in the 2D design are shown in Fig. 13(b).

Step 10: Fundamental period check

Using eigenvalue analysis in SAP2000, modal analysis was carried out to determine the fundamental period of the designed structure. If the new period from SAP2000 is the same as the assumed period from step 5 then the EBD methodology is complete. If the periods are not the same, the new period was used as the input for step 5 and steps 6-10 are repeated. These iterations were continued until the fundamental period converged. The design iterations for the 2D structure are shown in Table 1. The final EBD design for the 2D structure is shown in Table 2.

Step 11: Validate the design

The final step in the methodology is to validate the EBD by applying the selected ground motions from step 1 on the MDOF structure. Fig. 14(a) shows the interstory drift results (solid) with the ESFP results (dotted). Fig. 14(b) shows the maximum displacement results for the EBD methodology on the timber-steel hybrid structure, considering also the mechanical room at the roof (8-storey). When compared to the ESFP designed building, the results show the benefits of designing following the EBD approach. By designing the t-stub connections to dissipate the plastic energy based on the axial distribution, the interstory drift results approaches the target drift.

Results show that the EBD performed as expected with an interstory drift value less than 2%. Moreover, the target drift did not exceeded for the earthquakes. Therefore, the performance level desired was achieved. However, under

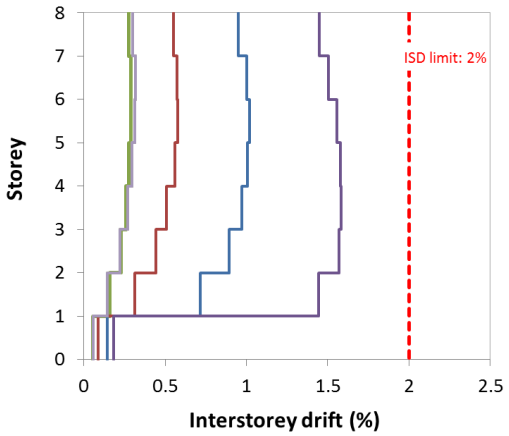

Fig. 14 NLTHA results in interstory drift (*y*-direction) for the EBD design

Table 3 Final EBD design details

CLT core walls	
Floors	Thickness (ply)
1 - 8	5
T-stub connections	
Floors	Type
1 - 7	H
0	E
Plate size	
Floors	Thickness (mm)
3 - 8	12
2	16
1	20

the proposed EBD methodology some of the earthquakes should have exceeded the target drift as the average acceleration values are less than the maximum ground motions. There are a variety of ways to calculate the input energy modification factor for the actual system. This research used the method proposed by Choi *et al*. (2006) for BRB framed structures. Modifying this equation for a lower ductility system will give more suitable results.

In the force based design a ductility of 2.0 was used as recommended by the CLT handbook. This was a conservative ductility as the handbook ductility was derived using a different structural system with less plastic deformation capacity. The value was chosen as no other study had been done on the timber-steel core wall system. The results show that a ductility of 2.0 was indeed conservative. Realistically, a larger ductility is more suitable for the proposed system. The ductility would be even larger if the building layout was less irregular as mentioned earlier. This is one of the main reasons PBSD was studied as the method does not rely on general seismic modification factors. There is just one ductility and overstrength value for a structural system in the NBCC. These modification factors do not change based on the structural layout or height. With PBSD the designer defines the target displacement and the ductility is determined based on the structural system, height and layout.

5. Conclusions

This paper examines a novel timber-steel core wall system for high seismic regions. The proposed hybrid timber-steel core walls were derived using first principles and validated with SAP2000. Results of the validation showed the timber-steel core walls were capable of resisting large overturning moments from seismic loads. The capacity of the system is adjusted by modifying the plate and *t*-stub connections and thickness of CLT panel. Confirming that the analytical model was behaving as designed; the model was used to analyze both the 2D and 3D performance of the structure under different design methodologies.

The timber-steel core wall system performed well in resisting the seismic forces from the earthquake ground motions on the studied building. The building plan irregularity had a large impact on the performance as the location of the cores were in opposite corners of the building. This irregularity resulted in the second two mode shapes being controlled by torsion. This structural layout restricted the performance of the building when compared to a building with core walls located on the same center line or with core walls in the center of the building. With less irregularity in the building layout the developed core wall system could be designed to deform more resulting in a smaller earthquake load due to the larger displacement ductility. The core wall system performed well under the building plan but has the ability to perform better with a less irregular layout as the t-stub connections can provide much more lateral displacement through plastic dissipation.

The following list outlines some aspects of the timber-steel core wall system and the proposed EBD methodology that need further study in order to ensure design application and feasibility.

1) Validate the derived lateral behaviour equations through experimental tests on the timber-steel core wall system.

2) Use finite element software that better captures the nonlinear behaviour of the t-stub connection. SAP2000 has limited hysteresis types; other software programs allow the user to define the hysteresis that would better dictate the nonlinear cyclic behaviour of the t-stub connection.

3) Consider various CLT panel configurations within the timber core wall system. Additional ductility could be introduced to the core system through friction or connections within the timber core wall connections.

4) Investigate the fire performance of the core system and modify the system to protect the steel elements in the CLT system.

5) Refine the EBD methodology. By extending the proposed EBD methodology to 3D it would better capture the behaviour of the timber-steel core system and allow for more robust design.

6) Test various layouts of the proposed core system. The building studied is irregular in shape, by considering a more high-rise style layout with one core wall area and smaller floor plan the strength and ductility of the system could be tested to its full extent.

Acknowledgments

The authors acknowledges the financial support from Natural Sciences and Engineering Research Council of Canada (NSERC) Engage grant program (EGP 476931-14) and Fast+Epp Structural Engineers for developing the timber-steel hybrid system.

References

Akiyama, H. (1985), *Earthquake-Resistant Limit-State Design for Buildings*, University of Tokyo Press.

Asiz, A. and Smith, I. (2011), "Connection system of massive timber elements used in horizontal slabs of hybrid tall buildings", *J. Struct. Eng.*, **137** (11), 1390-1393.

Atkinson, G.M. and Goda, K. (2011), "Effects of seismicity models and new ground-motion prediction equations on seismic hazard assessment for four Canadian cities", *Bull. Seismol. Soc. Am.*, **101**(1), 176-189.

Baker, J.W. (2011), "Conditional mean spectrum: Tool for ground motion selection", *J. Struct. Eng.*, **137**(3), 322-331.

Benavent-Climent, A. (2011), "An energy-based method for seismic retrofit of existing frames using hysteretic dampers", *Soil Dyn. Earthq. Eng.*, **31**(10), 1385-96.

Bezabeh, M. (2014), "Lateral behaviour and direct displacement based design of a novel hybrid structure: Cross laminated timber infilled steel moment resisting frames", M.A.Sc. Thesis, School of Engineering, University of British Columbia, Canada.

Bezabeh, M., Tesfamariam, S. and Stiemer, S., (2015b), "Equivalent viscous damping for steel moment-resisting frames with cross-laminated timber infill walls", *J. Struct. Eng.*, **142**(1), 04015080.

Bezabeh, M., Tesfamariam, S., Popovski, M., Goda, K. and Stiemer, S.F. (2017), "Seismic base shear modification factors for timber-steel hybrid structures: A collapse risk assessment approach", *ASCE J. Struct. Eng.*, **143**(10), 04017136-1-12.

Bezabeh, M., Tesfamariam, S., Stiemer, S., Popovski, M. and Karacabeyli, E. (2015a), "Direct displacement based design of a novel hybrid structure: steel moment-resisting frames with cross laminated timber infill walls", *Earthq. Spectra*, **32**(3), 1565-1585.

Blass, H.J. and Fellmoser, P. (2004), "Design of solid wood panels with cross layers", *Proceedings of the 8th World Conference on Timber Engineering*, Lahti, Finland, June.

Cheng, Y., Lucchini, A. and Mollaioli, F. (2014), "Proposal of new ground-motion prediction equations for elastic input energy spectra", *Earthq. Struct.*, **7**(4), 485-510.

Cheng, Y., Lucchini, A. and Mollaioli, F. (2015), "Correlation of elastic input energy equivalent velocity spectral values", *Earthq. Struct.*, **8**(5), 957-976.

Choi, H. and Kim, J. (2005), "Energy-based seismic design of buckling-restrained braced frames using hysteretic energy spectrum", *Eng. Struct.*, **28**, 304-311.

Choi, H. and Kim, J. (2009), "Evaluation of seismic energy demand and its application on design of buckling-restrained braced frames", *Struct. Eng. Mech.*, **31**(1), 93-112.

Choi, H., Kim, J. and Chung, L. (2006), "Seismic design of buckling-restrained braced frames based on a modified energy-balance concept", *Can. J. Civil Eng.*, **33**(10), 1251-1260.

CISC (2010), *Handbook of Steel Construction*, 10th Edition, CSA S16-09, Quadratone Graphics Ltd., Toronto.

CSI (2013), SAP2000 Linear and Nonlinear Static and Dynamic Analysis and Design of Three-Dimensional Structures: Basic Analysis Reference Manual, Berkeley, USA.

Decanini, L.D. and Mollaioli, F. (1998), "Formulation of elastic earthquake input energy spectra", *Earthq. Eng. Struct. Dyn.*, **27**, 1503-1522.

Decanini, L.D. and Mollaioli, F. (2001), "An energy-based methodology for the assessment of seismic demand", *Soil Dyn. Earthq. Eng.*, **21**(2), 113-137.

Dickof, C. (2013), "CLT infill panels in steel moment resisting frames as a hybrid seismic force resisting system", Masters Thesis, University of British Columbia.

Dickof, C., Stiemer, S.F., Bezabeh, M.A. and Tesfamariam, S. (2014), "CLT-steel hybrid system: ductility and overstrength values based on static pushover analysis", *ASCE J. Perform. Constr. Facil.*, **28**(6), A4014012.

Donaire-Á vila, J., Benavent-Climent, A., Lucchini, A. and Mollaioli, F. (2017), "Energy-based seismic design methodology: a preliminary approach", *16th World Conference on Earthquake Engineering, 16WCEE 2017*, Santiago Chile, January.

Donaire-Ávila, J., Mollaioli, F., Lucchini, A. and Benavent-Climent, A. (2015), "Intensity measures for the seismic response prediction of mid-rise buildings with hysteretic dampers", *Eng. Struct.*, **102**, 278-295.

Dowell, R.K., Seible, F. and Wilson, E.L. (1998), "Pivot hysteresis model for reinforced concrete members", *ACI Struct. J.*, **95**(5), 607-617.

FEMA (Federal Emergency Management Agency) (2009), "Quantification of building seismic performance factors", Technical Report P695, Applied Technology Council, Redwood City, California.

FEMA (Federal Emergency Management Agency) (2012), "Seismic performance assessment of buildings volume 1-methodology", Technical Report FEMA-P58, Washington, DC.

Fragiacomo, M., Dujic, B. and Sustersic, I. (2011), "Elastic and ductile design of multi-storey cross-lam massive wooden buildings under seismic actions", *Eng. Struct.*, **33**(11), 3043-3053.

Ghobarah, A. (2001), "Performance-based design in earthquake engineering: State of development", *Eng. Struct.*, **23**, 878-884.

Ghosh, S., Adam, F. and Das, A. (2009), "Design of steel plate shear walls considering inelastic drift demand", *J. Constr. Steel Res.*, **65**(7), 1431-1437.

Goertz, C. (2016), "Energy based seismic design of a multi-storey hybrid building: Timber steel core walls", Masters Dissertation, University of British Columbia.

Green, M. and Karsh, J.E. (2012), *Tall Wood-The Case for Tall Wood Buildings*, Wood Enterprise Coalition, Vancouver, Canada.

Hachem, M. (2004), "BISPEC: Bidirectional linear and nonlinear spectra of earthquakes", University of California, Berkeley, USA.

KLH (2012), "Technical characteristics of CLT", Retrieved from http://www.klhuk.com/media/29233/technicalcharacteristics.pdf

Leelataviwat, S., Goel, S.C. and Stojadinović, B. (2002), "Energy-based seismic design of structures using yield mechanism and target drift", *J. Struct. Eng.*, **128**(8), 1046-1054.

López-Almansa, F., Edgar Segués, E. and Cantalapiedra, I.R. (2015), "A new steel framing system for seismic protection of timber platform frame buildings. Implementation with hysteretic energy dissipators", *Earthq. Eng. Struct. Dyn.*, **44**(8), 1181-1202.

Loss, C., Piazza, M. and Zandonini, R. (2014), "Experimental tests of cross-laminated timber floors to be used in timber-steel hybrid structures", *World Conference on Timber Engineering*, Quebec City, Canada, August.

Loss, C., Piazza, M. and Zandonini, R. (2015a), "Connections for steel-timber hybrid prefabricated buildings. Part II: Innovative modular structures", *Constr. Build. Mater.*, **122**, 796-808.

Loss, C., Piazza, M. and Zandonini, R. (2015b), "Connections for

steel-timber hybrid prefabricated buildings. Part I: experimental tests", *Constr. Build. Mater.*, **122**, 781-795.
NRC (National Research Council Canada) (2010), "National Building Code of Canada", National Research Council of Canada, Ottawa, Ontario.
Pang, W. and Rosowsky, D.V. (2009), "Direct displacement procedure for performance-based seismic design of mid-rise wood-framed structures", *Earthq. Spectra*, **25**(3), 583-605.
Pei, S., van de Lindt, J., Popovski, M., Berman, J., Dolan, J., Ricles, J., Sause, R., Blomgren, H. and Rammer, D. (2014), "Cross-laminated timber for seismic regions: Progress and challenges for research and implementation", *J. Struct. Eng.*, **142**(4), E2514001.
Piluso, V. and Rizzano, G. (2008), "Experimental analysis and modelling of bolted T-stubs under cyclic loads", *J. Constr. Steel Res.*, **64**(6), 655-669.
Piluso, V., Faella, C. and Rizzano, G. (2001), "Ultimate behavior of bolted T-stubs. I: Theoretical model", *J. Struct. Eng.*, **127**(6), 686-693
Rinaldin, G., Amadio, C. and Fragiancomo, M. (2013), "A component approach for the hysteretic behaviour of connections in cross-laminated wooden structures", *Earthq. Eng. Struct. Dyn.*, **42**(13), 2023-2042.
Schneider, J., Karacabeyli, E., Popovski, M., Stiemer, S.F. and Tesfamariam, S. (2014), "Damage assessment of connections used in cross laminated timber subject to cyclic loads", *ASCE J. Perform. Constr. Facil.*, **28**(6), A4014008.
SEAOC Vision 2000 Committee (1995), Performance Based Seismic Engineering of Buildings, Sacramento, USA.
Shen, Y.L., Schneider, J., Tesfamariam, S., Stiemer, S.F. and Mu, Z.G. (2013), "Hysteresis behavior of bracket connection in cross-laminated timber shear walls", *Constr. Build. Mater.*, **48**, 980-991.
Smith, I. and Frangi, A. (2014), "Use of timber in tall multi-storey buildings", Structural Engineering Documents 13, International Association for Bridge and Structural Engineering.
Stiemer, S., Tesfamariam, S., Karacabeyli, E. and Propovski, M. (2012), "Development of steel-wood hybrid systems for buildings under dynamic loads", *STESSA 2012, Behaviour of Steel Structures in Seismic Areas*, Santiago, Chile, January.
Structurlam (2013), "Cross Laminated Timber Design Guide", Penticton, BC, Canada, http://structurlam.com/wp-content/uploads /2015/09/CLT-design-guide-metric-Sept-2015-low-res.pdf
Tesfamariam, S., Stiemer, S.F., Bezabeh, M., Goertz, C., Popovski, M. and Goda, K. (2015), "Force based design guideline for timber-steel hybrid structures : steel moment resisting frames with CLT infill walls", UBC Faculty Research and Publications.
Tesfamariam, S., Stiemer, S.F., Dickof, C. and Bezabeh, M.A. (2014), "Seismic vulnerability assessment of hybrid steel-timber structure: steel moment resisting frames with CLT infill", *J. Earthq. Eng.*, **18**(6), 929-944.
Uang, C.M. and Bertero, V.V. (1990), "Evaluation of seismic energy in structures", *Earthq. Eng. Struct. Dyn.*, **19**(1), 77-90.
Zhang, X., Fairhurst, M. and Tannert, T. (2015), "Ductility estimation for a novel timber-steel hybrid system", *J. Struct. Eng.*, **142**(4), E4015001.